



# OPEN Spatial correlations between summer ozone heatwave dual events and residents mental health in China

Rongjun Zeng<sup>1</sup>, Jinhui Zhao<sup>2</sup>✉, Yanxia Hu<sup>2</sup>, Liling Chu<sup>3</sup>, Shenwen Du<sup>3</sup>, Changzhun Zheng<sup>1</sup> & Chao He<sup>4</sup>✉

In the context of global warming, the frequency and intensity of extreme heat events have significantly increased. Elevated temperatures accelerate atmospheric photochemical reactions, resulting in higher ambient ozone (O<sub>3</sub>) levels. This convergence of heatwaves and elevated O<sub>3</sub> concentrations presents a dual threat to public health. This study analyzes surface ozone concentrations and heatwave data from the summers of 2013 to 2020 across China, integrating these with mental health data from the Chinese population. Using spatiotemporal analysis and econometric models, we investigate the spatiotemporal dynamics of ozone and heatwaves during Chinese summers and assess population exposure risks.

Our findings quantitatively elucidate the correlations between combined ozone-heatwave events and residents' mental health. By 2020, the number of days with high surface ozone, heatwave days, and heatwave events in China had risen by 16.15%, 26.32%, and 15.67%, respectively, with marked spatial heterogeneity and clustering patterns. Despite a slight decline in 2020, the population exposed to high ozone levels (> 160 µg/m<sup>3</sup>) and prolonged heatwave conditions (> 20 days) showed an overall upward trend. Furthermore, 57.95% and 20.91% of regions are projected to remain at risk from these combined hazards. As surface ozone and heatwave exposure risks escalate, the mental health burden on residents has intensified, with significant spatial disparities observed.

**Keywords** Ozone-heatwave, Dual events, Mental health, Spatial correlations, China

Surface ozone pollution and extremely high temperatures, as common climate pollution events, have been widely recognized for their health and ecological hazards. Ozone is harmful to human health, increasing the incidence and mortality of cardiovascular and respiratory diseases<sup>1,2</sup>, and adversely affecting plant growth and ecosystems<sup>3</sup>, even influencing global climate change<sup>4</sup>. Heatwaves are closely associated with regional droughts, fires, and other disasters<sup>5</sup>. The IPCC's Sixth Assessment Report states that the global surface temperature from 2011 to 2020 was 1.1 °C higher than that from 1850 to 1900, with the rate of temperature increase accelerating<sup>6</sup>. The frequency and intensity of heatwave events have increased, impacting ecosystems<sup>7</sup>, socio-economic development<sup>8</sup>, and directly endangering human health and safety<sup>9</sup>, particularly for the elderly, by increasing cognitive impairment<sup>10</sup> and affecting sleep time<sup>11</sup>.

In recent years, combined events (ozone heatwaves) caused by high concentrations of ozone and extremely high temperatures have frequently occurred in various parts of the world, including China<sup>12</sup>, the United States<sup>13</sup>, Europe<sup>14</sup>, and the Mediterranean islands<sup>15</sup>. Compared to individual events, the bidirectional intensification effect of the ozone-heatwave compound event is significant. On the one hand, the increase in heatwave events accelerates the photochemical reactions responsible for ozone formation and creates favorable weather conditions for ozone accumulation<sup>16</sup>, leading to a sharp rise in ozone concentration<sup>17,18</sup>. On the other hand, ozone reacts with temperature. As a greenhouse gas, it absorbs long-wave radiation from the surface<sup>19</sup> and inhibits the transpiration cooling function of vegetation, which intensifies the rise in temperature and forms a positive feedback cycle of "heatwave-ozone"<sup>20</sup>. This ultimately results in an increasing frequency of combined high-temperature heatwaves and surface ozone pollution<sup>13,21</sup>. In China, ozone-heatwave compound events differ from single ozone pollution events, which are mainly concentrated in northern industrial areas due

<sup>1</sup>Faculty of Resources and Environmental Science, Hubei University, Wuhan 430062, China. <sup>2</sup>Normal School, Hubei University, Wuhan 430062, China. <sup>3</sup>College of Resources and Environment, Yangtze University, Wuhan 430100, China. <sup>4</sup>Wuhan Documentation and Information Center, Chinese Academy of Sciences, Wuhan 430071, China. ✉email: zhaojh2004@hubu.edu.cn; he\_chao@whu.edu.cn

to photochemical reactions<sup>22</sup>, and single heatwave events, which are distributed in the southern regions and influenced by climatic conditions<sup>23</sup>. Ozone-heatwave compound events exhibit significant spatial aggregation characteristics, with the eastern region of China becoming a high-incidence area for such events<sup>24,25</sup>. Meanwhile, the frequency, intensity, and duration of ozone-heatwave compound events have shown a significant increasing trend, both in the past and the future<sup>18,26</sup>. Observational data indicate that since the beginning of the twenty-first century, the frequency and intensity of heatwave events in China have increased by nearly three times, and the co-occurrence probability with ozone pollution has risen by more than 30%. CMIP6 predicts that the future development scenarios of high energy consumption and high emissions could further exacerbate the combined extreme events of heatwaves and ozone pollution<sup>12</sup>.

In response to these growing threats, extensive research has investigated the spatial distribution, mechanisms, and health impacts of ozone-heatwave events. Huang et al.<sup>24</sup> examined the spatial distribution and mechanisms of ozone-heatwave co-occurrence in China's Greater Bay Area, identifying higher frequencies in central regions. Schnell et al.<sup>27</sup> reported frequent ozone-heatwave co-occurrences in the northeastern USA from 1999 to 2013, highlighting consistent spatial and temporal patterns in extreme events. Lu et al.<sup>25</sup> found that during the extreme heat of 2018, regional ozone pollution occurred simultaneously in North and East China, with over 63% of cities experiencing abnormally high ozone levels, closely related to local high-pressure and strong subsidence conditions. Li et al.<sup>12</sup> observed that cities with severe ozone pollution faced more frequent heatwaves, with persistent heat exacerbating ozone formation, as shown by field observations and climate-chemistry coupled simulations. These studies suggest that while the spatial distribution and formation mechanisms of ozone-heatwave compound events exhibit significant regional differences, there are commonalities in the meteorological conditions and the synergistic effects of chemical reactions.

Whether long-term and short-term exposure to ozone or heatwaves negatively impacts human health. Zhao et al.<sup>28</sup> investigated the spatial and temporal distribution of summer surface ozone and population exposure in Beijing from 2014 to 2016. The results showed that the ozone concentration decreased from north to south, while the number of people exposed to exceeding ozone standards reached 10.84 million, 9.73 million, and 10.54 million respectively from 2014 to 2016, accounting for 50.38%, 44.85%, and 48.49% of Beijing's population. Wang et al.<sup>29</sup> compared the heat hazards and heat exposure in Beijing and New York, finding that heat exposure in Beijing mostly occurred in areas with high population density and more elderly people, whereas in New York, it was more prevalent in areas with dense populations of poor people, and was related to urban greening coverage. This indicates that socio-economic and ecological factors jointly contribute to inequitable urban heat exposure. Wang et al.<sup>30</sup> predicted the future urban heatwave exposure under four shared socio-economic pathways (SSPs) and found that the risk of global urban population exposure to heatwaves increased across all SSPs. There were significant differences in the degree of exposure and inequality among countries with varying income levels. Additionally, similar studies have been conducted by Zhang<sup>31</sup>, Mitis<sup>32</sup>, Campbell<sup>33</sup>, and others.

It is worth noting that ozone-heatwave compound events have far greater adverse impacts on various aspects of the environment, health, and ecosystems with overlapping effects than single pollution events. In the ecological dimension, these events threaten the ecosystem's carbon balance by altering plant carbon allocation patterns<sup>34</sup>. In the socio-economic dimension, they increase socio-medical and economic burdens<sup>35</sup>, elevate urban energy consumption, exacerbate industrial high-energy consumption scenarios, and worsen economic losses<sup>12</sup>. Among these, the impact on the public health system is the most intense<sup>36</sup>, including direct physiological damage and indirect social service pressure. As for health risks, the enhancing effect of their adverse impacts far exceeds the simple superimposition of single events. The risk of all-cause mortality, circulatory system disease mortality, and respiratory system disease mortality due to compound events is higher than that associated with a single ozone-heatwave event<sup>12</sup>. In particular, it exacerbates the excess mortality risk from cardiovascular and cerebrovascular diseases in the elderly<sup>37</sup> and has a greater impact on the death risk of individuals with cardiopulmonary diseases. Therefore, understanding summer heatwave-ozone compound pollution is essential for addressing climate-related health risks.

Despite significant research on heatwaves and ozone, most studies have focused on individual events, with less research on ozone-heatwave complexes, their spatial and temporal correlations, exposed populations, and risks. Research on population exposure and risks is also primarily based on small urban areas, with large-scale regional studies relying on future simulations and predictions<sup>30,38</sup>. Thus, further studies on large-scale regional statistics on compound exposure risks are needed. Previous studies have shown that air pollution significantly impacts residents' psychological health, increasing anxiety, depression, and other mental health issues while reducing subjective well-being<sup>39,40</sup>. However, previous studies have focused more on the effects of compound events on residents' physical health, while the specific impact on residents' mental health and the differences in different regions have not yet been understood in sufficient depth.

This study, based on 2013–2020 summer surface ozone concentration data, heatwave data, population data, and residents' mental health data from China, employs spatial analysis, exposure risk assessment, and correlation analysis to explore the spatiotemporal evolution of surface ozone concentrations and heatwaves, population exposure, and their relationship with residents' mental health during the Chinese summer. It aims to reveal the impact and regional disparities of ozone-heatwave compound pollution on residents' mental health. The findings are crucial for guiding public health policies and interventions to mitigate the adverse effects of extreme climate events on mental health.

## Materials and methods

### Study area

This study takes all 34 provincial-level administrative regions in China as the research areas, analyzing the compound pollution scenarios of surface ozone concentrations and heatwaves from 2013 to 2020. Particular attention is paid to six major metropolitan agglomerations: Beijing-Tianjin-Hebei (BTH, primarily including

14 cities such as Beijing and Tianjin), Guanzhong Plain (GZP, mainly comprising 5 cities including Xi'an and Baoji), Central Plains (CPU, primarily including 14 cities such as Zhengzhou and Kaifeng), Yangtze River Delta (YRD, mainly including 27 cities such as Shanghai and Nanjing), Chengdu-Chongqing (CCQ, including 15 cities in Sichuan Province such as Chengdu and Nanchong, 27 districts and counties in Chongqing such as Yuzhong and Jiangbei, as well as parts of Kaizhou and Yunyang), and Pearl River Delta (PRD, mainly including 9 cities such as Guangzhou and Foshan). These urban agglomerations are not only China's main economic growth poles but also regions severely threatened by ozone pollution and heatwaves<sup>12,41,42</sup>. The specific details of these urban agglomerations are shown in Fig. 1.

### Data sources

The spatially continuous gridded daily maximum 8-hour average ozone concentration data from 2013 to 2020 at a resolution of 10 km were collected from the China Atmospheric Composition Real-time Tracking dataset (<http://tapdata.org.cn/>). Heatwave data for the same period were obtained using a combined threshold definition method from the Global Daily Apparent Temperature and Annual Heatwave dataset (<https://zenodo.org/records/4764325>). Events with a temperature constant threshold equal to 29 °C and a percentile threshold equal to 85% for three consecutive days are defined as heatwaves. Population data were derived from the WorldPop Global Population Grid dataset (<https://hub.worldpop.org/>). Resident mental health data were obtained from a dataset of the density distribution of MHQs in China based on a real-time Internet search engine studied by Zhou et al.'s team<sup>43</sup>. According to the research and definitions of the World Health Organization, this dataset focuses on two of the most common mental health issues: depression and anxiety. Seven keywords related to depression and eight keywords related to anxiety were translated into Chinese as relevant search terms. Then, combined with a regular expression (Regex =  $[A] * ! [B]$  where A is a set of selected keywords representing depression and anxiety, and B is a set of words used to exclude irrelevant queries), MHQs data were filtered out from the daily real-time search data in 252 cities in China, collected from the Baidu search engine, covering the period from March 1, 2019, to December 31, 2019, according to the filtering rules (if a search query contains at least one keyword from A and none of the words from B, it is considered a valid MHQ). Subsequently, correlation verification was conducted using the real mental-health-related cases (MHCs) from online doctor consultations collected by a leading online health care platform in China (Haodf), as well as the distribution of the top ten most common search queries most likely to reflect mental health issues. The results demonstrated a highly significant correlation, indicating that the MHQs data can reliably reflect the mental health status of residents. Ultimately, MHQs were aggregated at the city level, resulting in a dataset used to estimate the impact of both short-term and long-term exposure to air pollution on urban residents' mental health. A higher per capita MHQs value indicates poorer mental health status in the region.

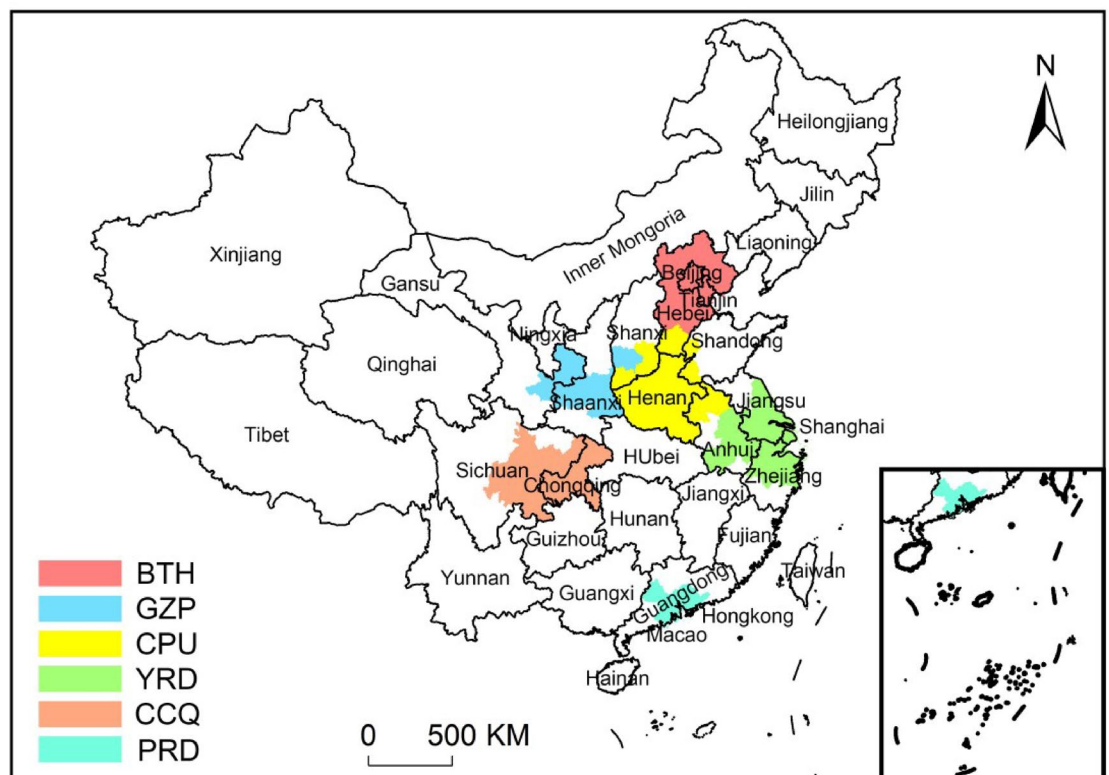


**Fig. 1.** Spatial distribution map of the study area and the six major urban agglomerations.

### Trend analysis

Trend analysis is a method of predicting the trend by performing linear regression analyses on time-varying variables. It is commonly applied in the temporal dynamic analysis of air pollutants to explore the interannual variation rate of pollutants<sup>44,45</sup>. This study employs trend analysis methods to examine the interannual variations and spatial patterns of summer surface ozone concentrations and the number of heatwave days and events in China from 2013 to 2020. The specific formula used for this analysis is as follows (Eq. 1):

$$Trend = \frac{n \times \sum_{i=1}^n (i \times P_i) - (\sum_{i=1}^n i) (\sum_{i=1}^n P_i)}{n \times \sum_{i=1}^n i^2 - (\sum_{i=1}^n i)^2} \quad (1)$$

where  $n$  represents the period (in this study,  $n=8$ );  $i$  is the specific year within the study period; and  $P_i$  denotes the value of summer surface ozone concentration, heatwave days, or events in the  $i$ -th year. The resulting slope indicates the trend of change: a positive slope suggests an increasing trend in summer surface ozone concentrations and heatwave metrics, whereas a negative slope indicates a decreasing trend.

### Spatial autocorrelation analysis

Spatial autocorrelation analysis assumes that the geographical locations of the study samples are interconnected. Through the identification of feature regions, it reveals the correlations of geographical elements in the spatial evolution process, including two parts: global spatial autocorrelation and local spatial autocorrelation. The Global Moran's  $I$  is an important index to reveal the degree of similarity in attribute values between adjacent regional units, while local spatial autocorrelation analysis uses local spatial connectivity indices to measure the significant spatial aggregation degree between the attribute values of each regional unit and its surrounding areas<sup>46,47</sup>. This study employs the Global Moran's  $I$  and Anselin Local Moran's  $I$  indices to explore the global and local spatial autocorrelations of summer surface ozone concentrations and heatwave metrics (days and events) in China from 2013 to 2020. These tools are used to identify spatial clustering and heterogeneity in the rates of change and correlations between surface ozone concentrations and heatwave metrics. The specific formulas are as follows (Eqs. 2 and 3):

$$I = \frac{n \sum_{i=1}^n \sum_{j=1}^n W_{ij} (x_i - \frac{1}{n} \sum_{i=1}^n x_i) (x_j - \frac{1}{n} \sum_{i=1}^n x_i)}{\sum_{i=1}^n \sum_{j=1}^n W_{ij} \sum_{i=1}^n (x_i - \frac{1}{n} \sum_{i=1}^n x_i)^2} \quad (2)$$

$$I_i = \frac{n (x_i - \bar{x}) \sum_{j=1}^n W_{ij} (x_j - \bar{x})}{\sum_{i=1}^n (x_i - \bar{x})^2} \quad (3)$$

where  $I$  represents the Global Moran's  $I$  index, and  $I_i$  represents the Anselin Local Moran's  $I$  index;  $n$  denotes the number of study units;  $x_i$  and  $x_j$  are the change rates of summer surface ozone concentrations, heatwave days, or heatwave events for study units  $i$  and  $j$ , respectively;  $\bar{x}$  is the mean change rate or correlation of all study units;  $W_{ij}$  is the spatial weight matrix between units  $i$  and  $j$ . Global Moran's  $I \in [-1, 1]$ , if Global Moran's  $I > 0$ , it indicates positive spatial autocorrelation; if Global Moran's  $I < 0$ , it indicates negative spatial autocorrelation; and if Global Moran's  $I \approx 0$ , it suggests no spatial autocorrelation,  $|Global\ Moran's\ I|$  with larger values indicating stronger correlations.

Using Local Moran's  $I$  and the standardized statistical Z-score  $Z(I)$ , four types of spatial clustering can be diagnosed: high-high, low-low, high-low, and low-high clustering<sup>48</sup>. The specific formula is as follows (Eq. 4):

$$Z(I) = \frac{I - E[I]}{\sqrt{V[I]}}, \quad E[I] = -\frac{1}{n-1}, \quad V[I] = E[I^2] - E[I]^2 \quad (4)$$

when  $I > 0$ , if  $Z(I) > 1.96$ , it signifies high-high clustering, where the area and its surrounding regions exhibit higher-than-average rates of change in summer surface ozone concentrations, heatwave days, or heatwave events. Conversely, it indicates low-low clustering, where the area and its surroundings show lower-than-average rates. When  $I < 0$ , if  $Z(I) > 1.96$ , it denotes high-low clustering, where a high-value area is surrounded by low-value areas; otherwise, it indicates low-high clustering.

### Hot and cold spot analysis

When the local spatial units have high-value and high-value clustering or low-value and low-value clustering, or when outliers are present within the study area, it is necessary to further analyze the spatial distribution pattern of attribute values within the area. The Getis-Ord  $G_i^*$  index is well-suited for this purpose, as it can effectively identify spatial clustering and dispersion patterns of the features under investigation<sup>49</sup>. This study employs the Getis-Ord  $G_i^*$  statistic to identify the spatial clustering of trends in summer surface ozone concentrations, heatwave days, and heatwave events in China from 2013 to 2020. The specific formula used is as follows (Eq. 5):

$$G_i^* (d) = \frac{\sum_{j=1}^n W_{ij} x_j - \bar{X} \sum_{j=1}^n W_{ij}}{S \sqrt{\frac{\sum_{j=1}^n W_{ij}^2 - (\sum_{j=1}^n W_{ij})^2}{n-1}}} \quad (5)$$

where  $x_j$  represents the change rate of summer surface ozone concentration, heatwave days, or heatwave events for study unit  $j$ ;  $w_{ij}$  is the spatial weight matrix;  $S$  is the standard deviation, and  $\bar{X}$  is the mean change rate or correlation of all study units;  $n$  denotes the number of study units. The computed Z-score from this formula indicates the nature of the spatial cluster: a positive Z-score signifies a hotspot, while a negative Z-score indicates a cold spot.

### Population exposure quantification

In this study, population data were first resampled in ArcGIS 10.8 to match the resolution of surface ozone and heatwave datasets based on the distribution characteristics of surface ozone concentrations and heatwaves in China. Subsequently, zonal statistics were employed to quantify the population exposed to varying levels of surface ozone concentrations and number of heatwave days<sup>50,51</sup>. To examine the temporal characteristics of population exposure, this study also calculated the cumulative proportion of the population exposed within different range intervals for each year from 2013 to 2020.

### Population exposure risk assessment

Population exposure risk is determined by the combined factors of environmental conditions related to ozone and heatwaves and the distribution of the population. To quantify the intensity of population exposure to surface ozone and heatwave environments in specific regions, this study incorporates a relative risk assessment model for population exposure<sup>52</sup>. This model calculates the ratio of grid-based population exposure risk to the average risk within the region, reflecting the severity of population exposure risk in regional subunits relative to the overall area. The specific formula is as follows (Eq. 6):

$$R_i = \frac{pop_i \times C_i}{\sum_{i=1}^n pop_i \times \frac{C_i}{n}} \quad (6)$$

where  $i$  represents the grid number,  $R_i$  denotes the relative risk of population exposure in grid  $i$ ,  $pop_i$  is the total population in grid  $i$ ,  $C_i$  represents the surface ozone concentration or the number of heatwave days in grid  $i$ , and  $n$  is the number of grids in the study area. To clearly and effectively assess the spatial distribution of relative risk of population exposure within the region, we will reclassify  $R_i$  in ArcGIS 10.8. The specific classification standards are as follows:  $R_i < 0$  indicates an extremely low-risk area (ELR),  $R_i \in (0, 1)$  a low-risk area (LR),  $R_i \in (1, 2)$  a lower-risk area (LRR),  $R_i \in (2, 3)$  a higher-risk area (HRR),  $R_i \in (3, 5)$  a high-risk area (HR), and  $R_i > 5$  an extremely high-risk area (EHR).

### Hurst index

The Hurst index can be used to describe and analyze the long-term memory characteristics of a time series, which is widely used to assess the strength of persistence or anti-persistence in the trends of time series changes<sup>53,54</sup>. In this study, we utilize the Hurst index to analyze the sustainability of the relative risk of population exposure. The specific formulas for calculation are as follows (Eqs. 7, 8, and 9):

$$X(t) = \sum_{i=1}^T (\Delta R_i - \overline{\Delta R(\theta)}) \quad 1 \leq t \leq \theta \quad (7)$$

$$R(\theta) = \max_{1 \leq T \leq N} X(t) - \min_{1 \leq T \leq N} X(t) \quad (\theta = 1, 2, \dots, n) \quad (8)$$

$$S(\theta) = \left[ \frac{1}{\theta} \sum_{i=1}^T (\Delta R_i - \overline{\Delta R(\theta)})^2 \right]^{1/2} \quad (\theta = 1, 2, \dots, n) \quad (9)$$

where  $R_i$  ( $i = 1, 2, 3, \dots, n$ ) represents the time series of calculated relative risks of population exposure to either ozone or heatwave days.  $T$  denotes any positive integer,  $\Delta R_i$  represents the difference series,  $\overline{\Delta R(\theta)}$  the mean series,  $R(\theta)$  the range, and  $S(\theta)$  the standard deviation.

## Results

### Spatiotemporal evolution patterns of summer surface ozone and heatwaves

From 2013 to 2020, the summer surface ozone concentrations in China experienced an initial increase followed by a decrease. It started at 85.98  $\mu\text{g}/\text{m}^3$  in 2013, peaked at 105.33  $\mu\text{g}/\text{m}^3$  in 2019, and slightly decreased to 102.54  $\mu\text{g}/\text{m}^3$  in 2020 (Fig. 2a). The number of heatwave days and events was divided into two phases around 2016: a sharp increase phase (2013–2016) and a slow decline phase (2016–2020). During Phase I, heatwave days and events increased by 67.81% and 44.17%, respectively; in Phase II, they decreased by 24.69% and 19.85% (Fig. 2b,c). Spatially, summer surface ozone concentrations increased in about 96% of China, with annual growth rates ranging from 0 to 14.07  $\mu\text{g m}^{-3} \text{ yr}^{-1}$ . Regions with an annual change rate exceeding 3.29  $\mu\text{g m}^{-3} \text{ yr}^{-1}$  were mainly concentrated in North China, East China, and the southwest of Northwest China. The spatial distribution of heatwave days and events also showed similar increasing trends, particularly pronounced in the eastern, southern, and certain inland northwestern regions. In the southeastern areas, the rate of change in heatwave days exceeded 1.62 days/year, and the rate of change in heatwave events surpassed 0.22 times/year. In contrast, regions with reductions in heatwave days and events were mainly located in the Central Plains and the western part of the country, such as the western Tarim Basin and central Junggar Basin (Fig. 2d–f).

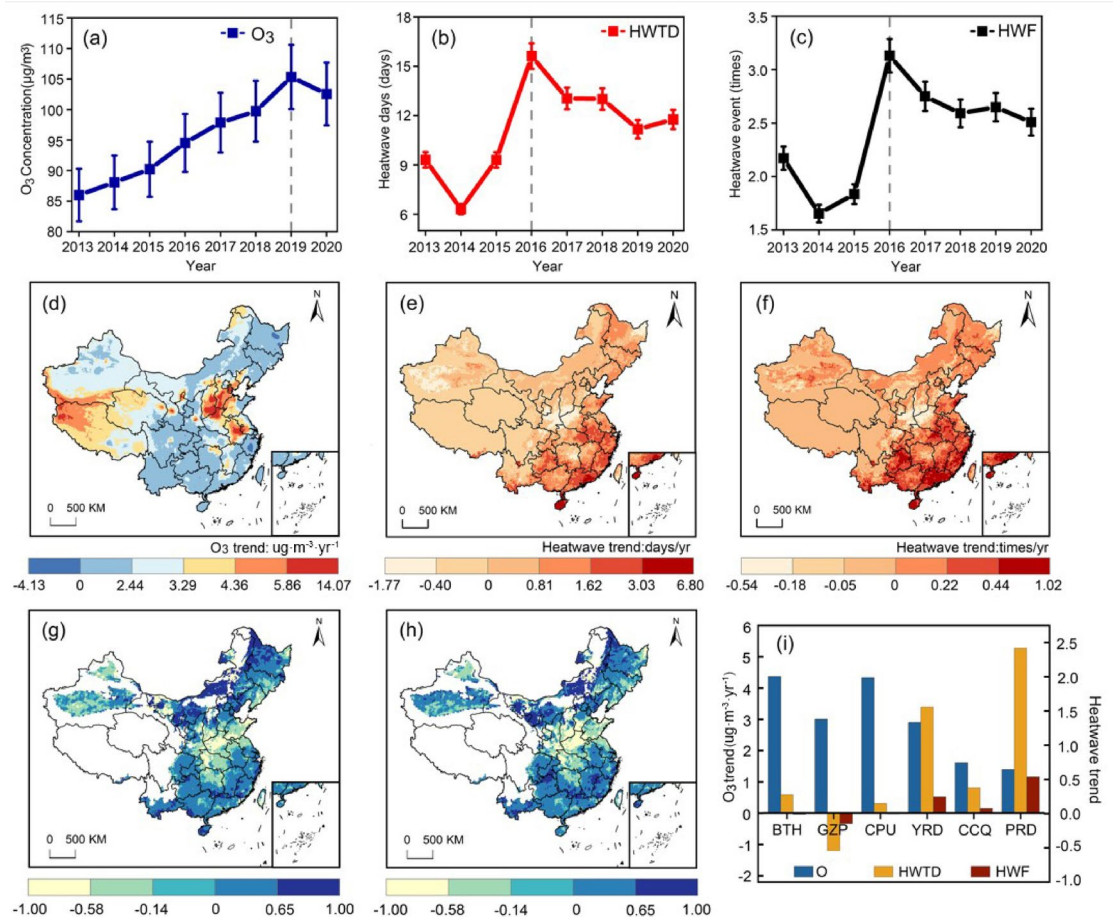


**Fig. 2.** Spatiotemporal evolution patterns of summer surface ozone concentrations and heatwaves. (a–c) Time series of annual average summer surface ozone concentrations and the number of heatwave days and events from 2013 to 2020, with the peak year and its corresponding values indicated by gray dashed lines; (d–f) Spatial distribution of the trends in summer surface ozone concentrations and the number of heatwave days and events from 2013 to 2020; (g–h) Spatial correlations between summer surface ozone concentrations and the number of heatwave days and events from 2013 to 2020; (i) Trends in summer surface ozone concentrations and the number of heatwave days and events from 2013 to 2020 across China's six major urban agglomerations.

Among the six urban agglomerations, summer surface ozone concentrations showed an increasing trend, with the Beijing–Tianjin–Hebei and Central Plains urban agglomerations exhibiting the most remarkable annual growth rates of  $4.37 \mu\text{g m}^{-3} \text{ yr}^{-1}$  and  $4.33 \mu\text{g m}^{-3} \text{ yr}^{-1}$ , respectively. Except for a declining trend in heatwave days in the Guanzhong Plain urban agglomeration (average decrease of 0.54 days/year), the other urban agglomerations showed increasing trends, with the highest annual growth rate in heatwave days observed in the Pearl River Delta urban agglomeration at 2.42 days/year. The heatwave event numbers slightly decreased in the Beijing–Tianjin–Hebei, Guanzhong Plain, and Central Plains urban agglomerations, while other agglomerations experienced increases, with the highest annual growth rate of 0.54 times/year in the Pearl River Delta urban agglomeration (Fig. 2i). The correlation between summer surface ozone concentrations and the number of heatwave days and events was predominantly positive across most regions, especially in the north-eastern region, central-eastern Inner Mongolia and the southern part of the country, where the correlation ranged from 0.65 to 1. The negative correlation areas were mainly in southern North China, Central China, central Inner Mongolia, and the border of Northeast China, ranging from  $-1$  to  $-0.58$  (Fig. 2g,h).

Figure 3 displays the spatiotemporal clustering results of ozone and heatwaves during the study period. We found significant spatial similarities in the clustering patterns of changes in surface ozone concentrations and the number of heatwave days and events. Specifically, the global Moran's  $I$  for the change rates of surface ozone concentrations, heatwave days, and heatwave events was significant at the 1% level, indicating a strong positive spatial correlation in the trends. Furthermore, the distribution of hot and cold spots for surface ozone concentration trends and heatwave events closely resembled their respective high-high and low-low clustering areas. Hotspot and high-high clustering areas for surface ozone concentration trends were primarily distributed in North China, northern East China, and the central-western regions of the Tibetan Plateau, while those for heatwave days were mainly along the southeastern coast and small parts of the northeast. At the same time,

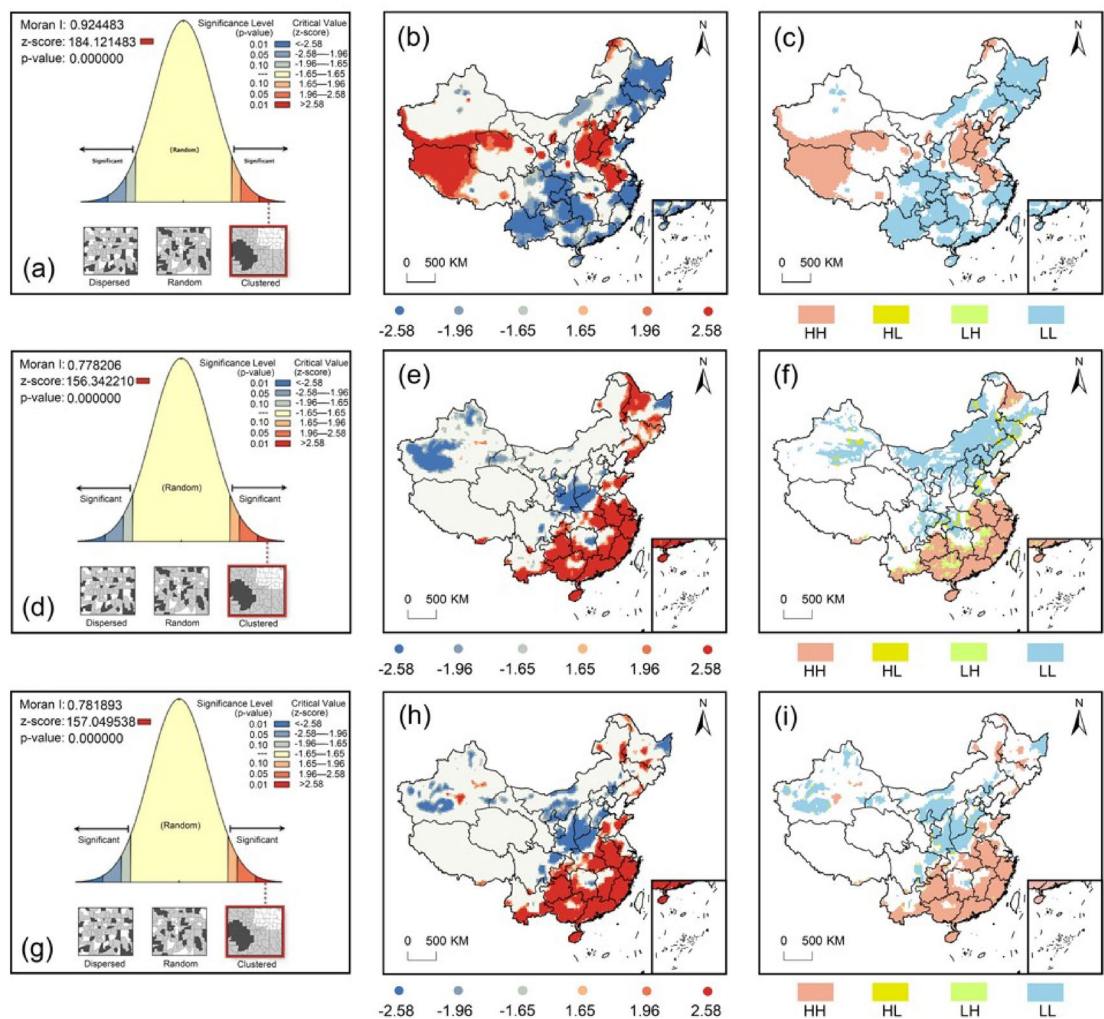


**Fig. 3.** Spatial clustering characteristics of summer surface ozone and heatwaves spatiotemporal evolution from 2013 to 2020. (a), (d), and (g) are Global Moran's  $I$  for the trends in summer surface ozone concentrations and the number of heatwave days and events; (b), (e), and (h) are the spatial distribution of hot and cold spots for the trends in summer surface ozone concentrations and the number of heatwave days and events; (c), (f), and (i) are the spatial distribution of spatial clustering for the trends in summer surface ozone concentrations and the number of heatwave days and events.

	Low heatwaves	Moderate heatwaves	High heatwaves
Low $O_3$	Southwest China, Northeast China	Northeast China, Southwest China, Southeast China	Southeast Coastal Region, Southwest China
Moderate $O_3$	Tibetan Plateau, Northwest China	Northeast China, Inland Northwest, Central-Eastern China	Southeastern China
High $O_3$	Western and Central Tibetan Plateau, North China	North China, East China	Eastern China West

**Table 1.** Spatial evolution of ozone-heatwave compound events.

the hot and cold spot distribution areas for heatwave days and events were largely consistent. The difference is that heatwave days have more significant high-low and low-high cluster type regions, scattered around the periphery of the low-low and high-high clustering distribution areas.

Table 1 represents the results of the spatial evolution of surface ozone-heatwave compound events during the summer. We observed significant spatial distribution differences among different types of ozone-heatwave compound events throughout the study period, with some event types exhibiting similar spatial distribution patterns. High  $O_3$ -low heatwaves and moderate  $O_3$ -low heatwaves compound events are predominantly distributed across the Tibetan Plateau, Northwest China, and North China, with a relatively large and continuous spatial distribution. In contrast, high  $O_3$ -high heatwaves, high  $O_3$ -moderate heatwaves, moderate  $O_3$ -high heatwaves, and low  $O_3$ -high heatwaves compound events have a smaller spatial distribution area, but their clustering distribution characteristics are prominent, with these events mainly concentrated in the eastern

and southern regions of China. Moderate  $O_3$ -moderate heatwaves, low  $O_3$ -moderate heatwaves, and low  $O_3$ -low heatwaves compound events are distributed in the northeast, southwest, inland northwest, and east-central regions of China, exhibiting significant discrete distribution characteristics. These findings suggest that ozone-heatwave compound events are becoming increasingly severe in the eastern part of the country.

### Population exposure risk for surface ozone and heatwaves

From 2013 to 2020, the proportion of the population exposed to summer surface ozone concentrations exceeding  $160 \mu\text{g}/\text{m}^3$  increased significantly from 0.19% in 2013 to 26.17% in 2019, then decreased to 16.50% in 2020. Concurrently, the proportion of the population exposed to an annual average of more than 20 heatwave days rose from 13.71% in 2013 to 46.24% in 2016, then gradually decreased to 24.17% in 2020 (Fig. 4a and f). Spatially, the land area exposed to ozone above the high-risk threshold (HRR) decreased from 9.91% in 2013 to 9.53% in 2016, further to 9.24% by 2020. These areas are primarily situated in the Beijing-Tianjin-Hebei, Central Plains, Yangtze River Delta, and Chengdu-Chongqing urban clusters. The land area exposed to ozone below the low-risk threshold (LRR) increased from 90.08% in 2013 to 90.75% in 2020, predominantly in the northwest and northeast regions. Overall, the risk of ozone exposure changed little in most parts of China (Fig. 4b–d). Similarly, the area exposed to heatwaves above the HRR decreased from 11.43% in 2013 to 10.68% in 2016, continuing to decline to 9.54% by 2020. These areas are mainly in the southern part of North China, Central China, the northeastern part of East China, and southern regions. In contrast, the area below the heatwave LRR increased from 88.57% in 2013 to 89.32% in 2016, continuing to rise to 90.46% by 2020, mainly distributed in the eastern and northwestern inland areas of China (Fig. 4g–i).

From the perspective of sustainable risk exposure, 57.95% and 20.91% of regions showed sustainability of population exposure risk to summer surface ozone and heatwaves in the future, respectively. This suggests that the pattern of population exposure risk to summer surface ozone and heatwaves observed from 2013 to 2020 may persist in these regions. Conversely, regions with anti-sustainability exposure risks were primarily located

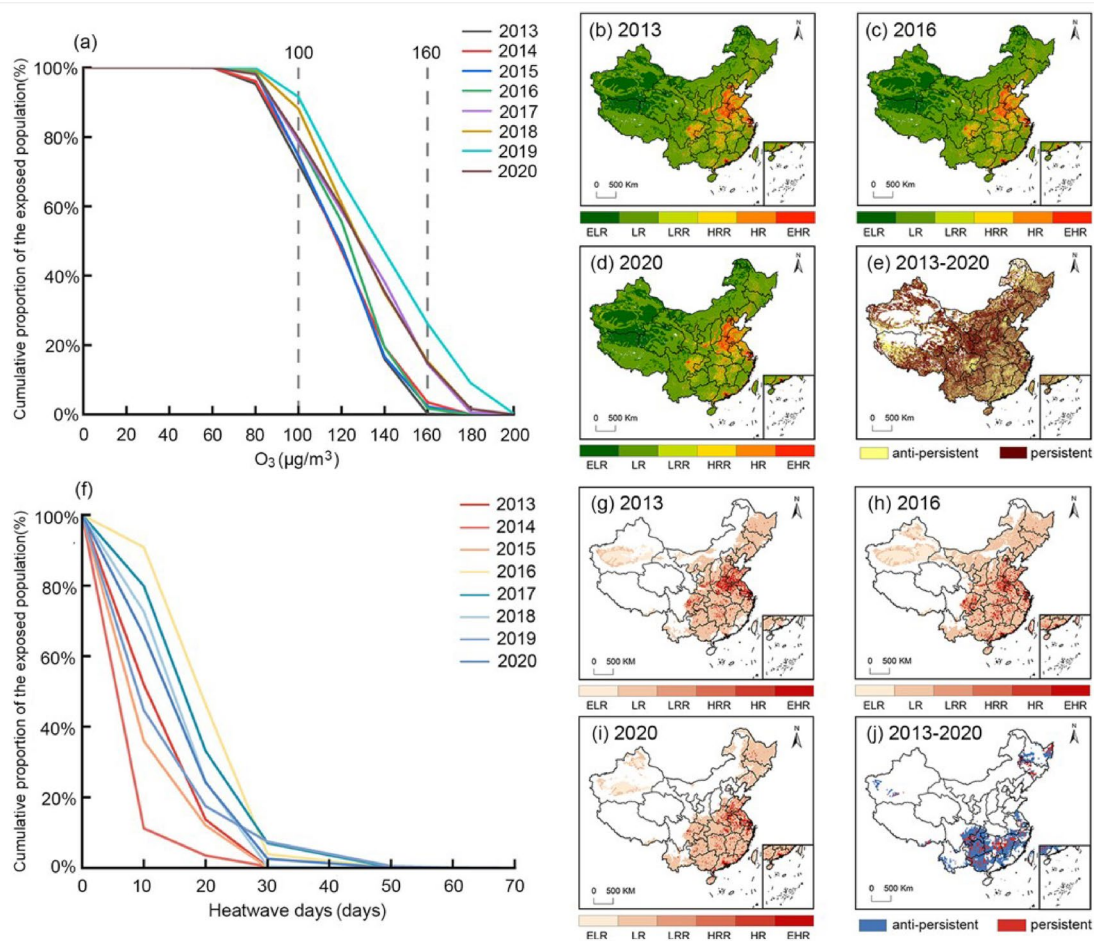


**Fig. 4.** Population exposure risk maps for surface ozone and heatwaves from 2013 to 2020. (a) and (f) Cumulative population exposure to varying summer surface ozone concentrations and heatwave days; (b–d) Average population exposure risk coefficients for summer surface ozone concentrations in 2013, 2016, and 2020; (e) Spatial distribution of the Hurst index for summer surface ozone concentrations; (g–i) Average population exposure risk coefficients for heatwave days in 2013, 2016, and 2020; (j) Spatial distribution of the Hurst index for heatwave days.

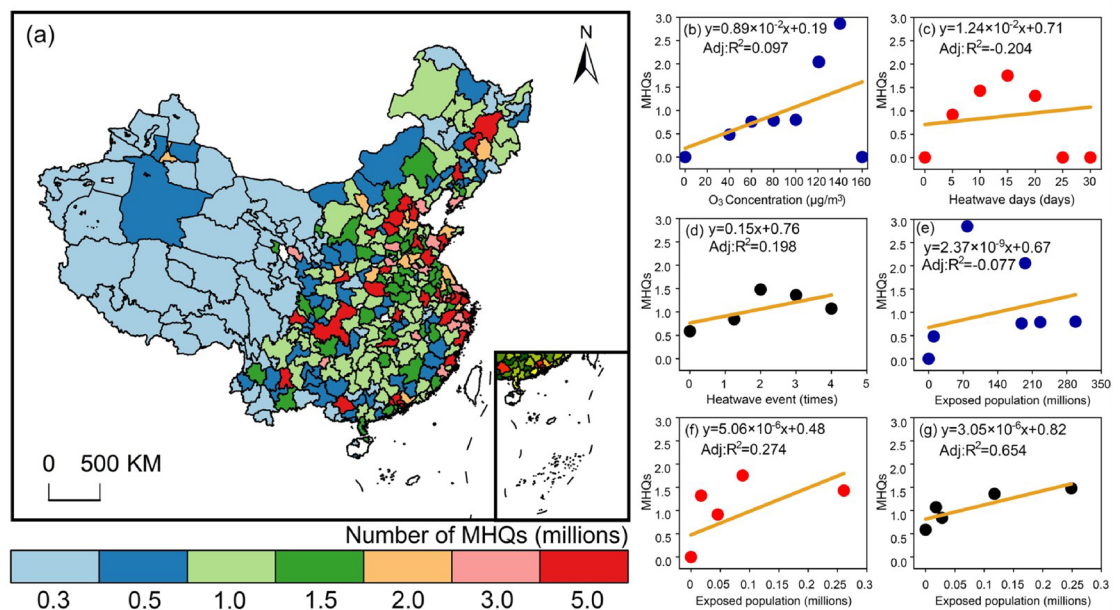
in eastern and southeastern China, comprising 42.05% and 79.09% of the study area, respectively. These places are less stable due to extensive human activity and frequent economic activity, and the future tendency may be the contrary from 2013 to 2020 (Fig. 4e and j).

### Spatial correlation characteristics with the mental health of the residents

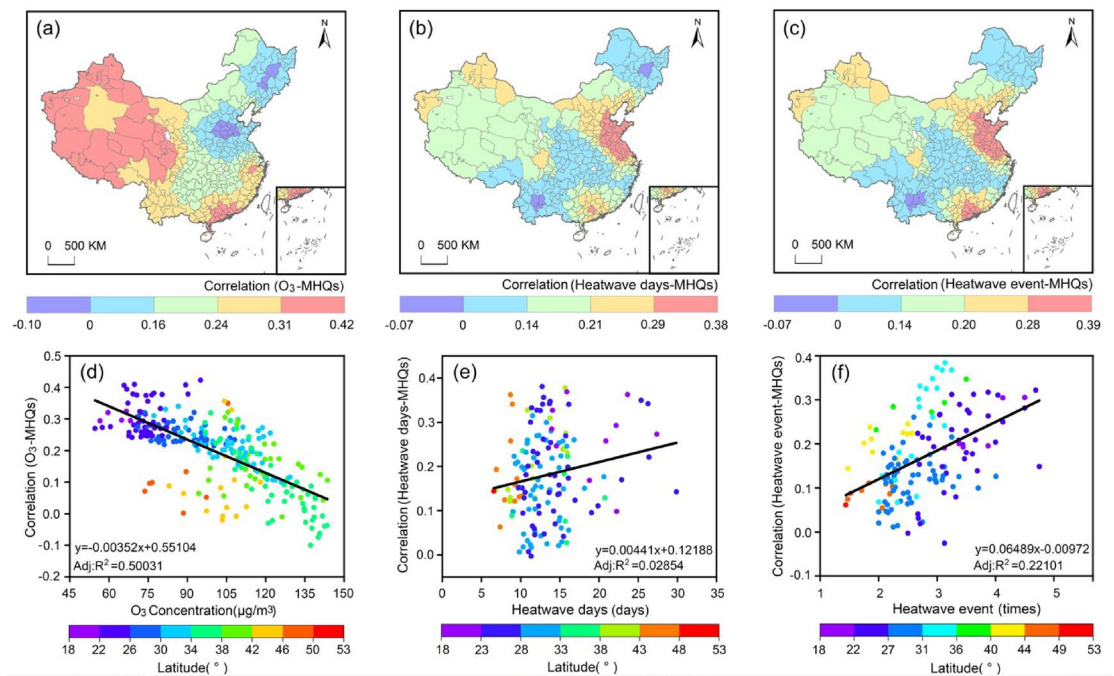
Figure 5 presents the spatial distribution of MHQs in China. The spatial distribution revealed a pattern of higher MHQs in the eastern regions and lower in the west, indicating poorer mental health status among residents in the east compared to those in the west. In the western regions, the distribution of MHQs was relatively uniform, mostly ranging between 0 and 0.5, whereas the eastern regions displayed a more complex distribution of MHQs values between 0.5 and 5.0, with high-value areas sporadically distributed, particularly prominent in the southeastern coastal areas (Fig. 5a). Among the six major urban clusters, the Beijing–Tianjin–Hebei (2.68 millions), Yangtze River Delta (2.66 millions), and Pearl River Delta (3.0 millions) urban clusters were the centers with high MHQs values. Notably, cities like Beijing (> 5.0 millions), Tianjin (> 5.0 millions), Baoding (3.0–5.0 millions), Shijiazhuang (3.0–5.0 millions) in the Beijing–Tianjin–Hebei cluster, Nanjing (> 5.0 millions), Suzhou (> 5.0 millions), Wuxi (> 5.0 millions), Shanghai (> 5.0 millions), Hangzhou (> 5.0 millions), Ningbo (> 5.0 millions), Hefei (3.0–5.0 millions), Jinhua (3.0 millions) in the Yangtze River Delta, and Guangzhou (> 5.0 millions), Shenzhen (> 5.0 millions), Dongguan (3.0–5.0 millions), Foshan (3.0–5.0 millions) in the Pearl River Delta were particularly notable, with MHQs all above 3.0 millions, and in some cities even higher than 5.0 millions.

Figure 5b–d show the linear regression relationships between different concentrations of ozone and the number of heatwave days and events with MHQs. We found that the surface ozone concentrations, heatwave days, and heatwave events during the Chinese summer were positively correlated with the mental health status of residents (Fig. 5b–d). The correlation with ozone was the most significant, with a correlation coefficient of 0.89. As ozone concentrations increased, MHQs rose, indicating a deterioration in residents' mental health status (Fig. 5b). In contrast, the positive correlations between heatwave days and heatwave events with MHQs were weaker. Notably, after reaching 15 heatwave days or 2 heatwave events, there was a slight decline in MHQs, suggesting that the increase in the number of heatwave days and heatwave events within these thresholds exacerbates mental health deterioration. However, once the cumulative number of heatwave days reached 15 or the number of events reached 2, their impact on mental health diminished, and residents' mental health may even have shown improvement (Fig. 5c and d).

During the study period, the population exposed to different ozone concentrations, heatwave days, and heatwave events also showed a positive correlation with MHQs (Fig. 5e–g). Specifically, for ozone, when the number of exposed individuals was between  $70 \times 10^6$  and  $210 \times 10^6$ , MHQs peaked (ranging from 2.0 to 3.0), indicating the poorest mental health status. Once the number of exposed individuals exceeded this range, MHQs decreased, suggesting an improvement in residents' mental health. In terms of heatwave days and heatwave events, changes in the number of exposed individuals did not significantly affect MHQs, and the mental health status remained relatively stable. For instance, when approximately  $0.08 \times 10^6$  individuals were exposed to a



**Fig. 5.** Spatial distribution of MHQs in China and scatter plots of correlation between ozone, heatwaves, and MHQs. (a) Spatial distribution of MHQs in China; (b–d) Correlation between summer surface ozone concentrations and the number of heatwave days and events with MHQs from 2013 to 2020; (e–g) Correlation between the number of exposed populations to summer surface ozone concentrations, heatwave days, and heatwave events with MHQs from 2013 to 2020.



**Fig. 6.** Spatiotemporal correlation features between surface ozone, heatwaves, and residents' mental health. (a–c) Spatial distribution of the correlation between summer surface ozone concentrations, heatwave days, and heatwave events with MHQs from 2013 to 2020; (d–f) Correlation coefficients between MHQs and summer surface ozone concentrations, heatwave days, and heatwave events, and their respective correlations with summer surface ozone concentrations and the number of heatwave days and heatwave events from 2013 to 2020.

certain number of heatwave days, MHQs reached their highest (between 1.5 and 1.8), corresponding to the worst mental health status. Beyond this number of exposed individuals, MHQs and the mental health status tended to stabilize. Similarly, when the population exposed to a certain number of heatwave events exceeded  $0.1 \times 10^6$ , the variation in MHQs was minimal (ranging from 1.0 to 1.5), indicating a stable mental health condition.

Further investigation into the spatial and temporal association characteristics between summer surface ozone concentrations, heatwave days, and heatwave events with MHQs in China from 2013 to 2020 revealed a generally positive correlation across most regions. However, spatial heterogeneity was also evident (Fig. 6a–c). Specifically, the correlation between summer surface ozone concentrations and MHQs showed a negative correlation (–0.10 to 0) only in the central part of North China and some cities in the central part of Northeast China, while the rest of the region showed a positive correlation (0 to 0.42) (Fig. 6a). Meanwhile, as surface ozone concentrations increased, the strength of the correlation between ozone and MHQs gradually decreased. The relationship between surface ozone concentrations and their correlation with MHQs exhibited a positive trend in low latitudes (18–30°N) of China. At the same time, the difference was obvious in the mid-latitude regions (30–53°N), with the most significant change in the 34–42°N region, where a positive–negative correlation existed in all regions (Fig. 6d).

There were similarities in the spatial and temporal correlation characteristics between the number of heatwave days and events and residents' mental health. The negative correlation between heatwave days and MHQs was only found in some cities in the northeast and a small part of the southwest (–0.07 to 0), while the positive correlation was found in the rest of the regions (0 to 0.38), particularly in the eastern part of North China, northern East China, and a few areas in South China, where the correlation coefficients were greater than 0.29 (Fig. 6b). Similarly, heatwave events exhibited a negative correlation only in a few areas in the southwest (–0.07 to 0), roughly matching and slightly expanding the negatively correlated areas shown for heatwave days. The rest of the regions exhibit positive correlations (0 to 0.39), with high positive correlation areas corresponding to and slightly expanding beyond those for heatwave days (Fig. 6c). With the increase in heatwave days and events, the strength of their correlation with MHQs also gradually increased. Compared to heatwave days, heatwave events showed a stronger correlation with MHQs. At different latitudes, the correlations were almost uniformly positive, especially at some mid-latitudes (31–40°N), where the positive correlation with MHQs was significant following the increase in heatwave events (Fig. 6e,f).

## Discussion

### Spatiotemporal evolution characteristics of surface ozone and heatwaves

This study comprehensively explored the spatial and temporal evolution characteristics of summer surface ozone and heatwaves in China from 2013 to 2020. In general, during the study period, summer surface ozone

concentrations, heatwave days, and heatwave events all exhibited an increasing and then decreasing trend. The slight decline in ozone concentrations after 2019 could be associated with reduced emissions and improved meteorological conditions in areas affected by the pandemic. There was also significant spatial heterogeneity in the trends of the three across the study area. Most of the nation had seen an increase in ozone concentrations, especially in North and East China and the southwest portion of the Northwest region. The primary causes of this are the high population density and frequent human activity, the advanced economic development and industrialization, the strong traffic demand, and the intense solar radiation in these regions<sup>55</sup>. This is because nitrogen oxides (NO<sub>x</sub>) and volatile organic compounds (VOCs), the key precursors for ozone formation, are extremely easy to produce under these conditions. Furthermore, there is a correlation between the general rise in surface ozone concentrations and the fall in atmospheric particulate matter concentrations, such as PM<sub>2.5</sub>. The chemical properties of particulate matter can absorb atmospheric hydroperoxyl radicals (HO<sub>2</sub>) and nitrogen oxides (NO<sub>x</sub>), both of which are crucial precursors required for ozone generation. Thus, with the recent reduction in particulate matter concentrations in China, ozone formation reactions have occurred more frequently. This finding is also consistent with an earlier study by Liao et al.<sup>56</sup>. The increasing trends in heatwave days and events are most noticeable in the southeastern region, closely related to the low latitude, tropical or subtropical monsoon climate, rapid urbanization, dense population distribution, and well-developed industry.

Investigating the correlation between surface ozone concentrations and the number of heatwave days and events revealed that, in most regions of China, surface ozone levels were positively correlated with both heatwave metrics. This correlation primarily stems from elevated temperatures enhancing the rate of photochemical reactions, thereby increasing ground-level ozone concentrations as temperatures rise. This finding aligns with previous research that has similarly observed these trends<sup>15,57</sup>. However, in this study, the correlation between surface ozone concentrations and heatwave days and events showed a negative trend in central and eastern China (southern North China and Central China regions). This could be because increased atmospheric temperatures enhance the chemical reaction rates, leading to more ozone formation from NO<sub>x</sub> and VOCs under sunlight. However, as temperatures continue to rise, the atmospheric stability layer usually becomes more unstable, causing pollutants at the surface to disperse upward, thereby reducing ground-level ozone concentrations. Thus, during heatwaves, despite the chemical tendency to increase ozone, ground-level concentrations might show a decreasing trend due to the effects of the atmospheric stability layer. Overall, our findings underscore the need for region-specific analysis and the adoption of targeted pollution control measures that consider the interplay between different pollutants and extreme events.

### Impact of ozone and heatwaves on residents' mental health

The results of the study on the impacts of surface ozone, heatwave days, and heatwave events on the mental health of residents showed that frequent surface ozone pollution and heatwaves lead to deteriorating mental health conditions. As pollution levels and the frequency of extreme events continue to rise, the mental health of residents becomes poorer and poorer. The correlations between these factors and mental health exhibit notable spatial heterogeneity, which is not only influenced by regional variations in extreme climatic events and pollution levels but also by differences in socio-economic factors such as population density and age structure, economic development, industrial composition, public health conditions, infrastructure, and the extent of green space in each region<sup>43</sup>.

A substantial body of previous empirical research has demonstrated that socio-economic factors can influence residents' mental health through two paths: material conditions (such as economic development level, industrial structure, etc.) and socio-environmental conditions (such as infrastructure, population density, etc.), either positively contributing to or posing a negative risk to mental health. Specifically, in terms of material conditions, areas with a high level of economic development tend to have higher overall income levels, which provide residents with sufficient financial resources to improve their living environment, access medical services, and engage in leisure and recreational activities, all of which benefit mental health<sup>58</sup>. In contrast, low-income and economically disadvantaged groups are prone to life stress, social exclusion, and a lack of health resources, thus increasing the risk of negative mental health<sup>59,60</sup>. It is also important to note that income fluctuations affect residents' mental health, with sudden income declines having a greater negative impact on mental health than sudden increases in income<sup>61</sup>. Furthermore, the regional industrial structure indirectly affects residents' mental health by influencing employment opportunities, income level, working environment, and the broader ecological environment<sup>62</sup>. In terms of socio-environmental conditions, well-developed infrastructure continues to play a positive role in promoting mental health in daily life, while the opposite will exacerbate residents' physical and mental fatigue<sup>63,64</sup>. For example, abundant green spaces and sports facilities provide residents opportunities for daily leisure and exercise, improving subjective well-being<sup>65,66</sup>. Adequate health resources enable early prevention and timely treatment of mental health issues<sup>67,68</sup>. Efficient transportation networks reduce commuting stress and mitigate psychological problems associated with air pollution and noise exposure<sup>69</sup>. A well-planned and high-quality distribution of commercial, cultural, educational, healthcare, and other public service facilities ensures residents' access to essential services, thereby reducing the risk of mental health issues arising or worsening<sup>70</sup>. In addition, along with the deepening process of urbanization, a large number of people enter the city to live and work, which can lead to adverse effects such as high population density, aggravation of the heat island effect, and serious environmental pollution, increase the sense of urban congestion, cause infrastructure overload, reduce the quality of the living environment of the residents, and damage the mental health of the residents<sup>71,72</sup>.

When extreme climatic events and pollution occur, these factors will also have a moderating effect on the impact of extreme weather events and pollution on residents' mental health. Favorable socio-economic conditions can mitigate the negative impacts of extreme climatic events and pollution, whereas unfavorable socio-economic conditions, compounded by extreme weather and pollution, may amplify the detrimental effects on mental health.

As our research has shown, there is a negative correlation between surface ozone concentrations and MHQs in northern and central-eastern China, while a strong positive correlation is observed in the inland regions of western China and the coastal regions of southern China. This pattern may be linked to the underlying influence mechanisms discussed above. In North and Northeast China, the high level of economic development and the availability of sufficient health resources make it easier for residents to access professional medical services when faced with the adverse impacts of air pollution and extreme events. This effectively mitigates the incidence of mental illnesses. Moreover, the region's long history of development and excellent infrastructure—such as efficient transport networks, diverse sports facilities, and abundant green spaces—provide residents with high-quality exercise and living space, which positively contribute to their mental health and help alleviate the negative effects of air pollution and extreme events.

In contrast, the coastal region of South China, despite having a similarly long development history, a robust economy, and relatively good infrastructure, exhibits a positive correlation between surface ozone concentrations and MHQs. This can be attributed to the fact that the region is mainly dominated by secondary and tertiary industries, particularly labor-intensive and service-oriented sectors, which have led to a large influx of migrant workers, extremely high population density, and an overstressed infrastructure. Along with rapid urbanization, various urban ailments have become notable, ultimately leading to a reduction in the standard of living environment and social and public health services enjoyed by the residents. Coupled with high work intensity, this has amplified daily life stress, which is detrimental to mental health. Consequently, when the region faces extreme climate events and air pollution, these factors further exacerbate the negative impacts, and the mental health of residents is increasingly at risk. For the western inland region of China, its relatively short development history, underdeveloped socio-economic conditions, and incomplete infrastructure have resulted in insufficient material conditions and social resources to safeguard residents' mental health. In addition, the current transfer of industries from the eastern part of China to the western part of the country primarily involves high-energy, high-emission, and high-pollution industries, which pose a significant threat to the already fragile ecological environment, thereby reducing residents' living quality. As a result, when residents in these areas face air pollution and extreme events, the negative impacts are further magnified, leading to increasingly severe mental health conditions.

In the face of increasingly frequent heatwaves, residents in the eastern part of North China, the northern part of East China, and small areas of South China experience the most significant adverse effects. On the one hand, some regions spanning the temperate and subtropical zones are influenced by the East Asian subtropical high from June to August each year. The intense continental radiative heating and the subsidence warming near the ridge line of the high lead to sharp increases in temperature, clear skies, and strong solar radiation, resulting in successive or intermittent extreme hot weather<sup>73</sup>. On the other hand, these areas are located along the central coast of China, connecting the economic and political centers of the country, with high traffic pressures. At the same time, with continuous economic development, increased industrial emissions, rapid urbanization, rising population size, expanding urban area, and the intensification of the urban heat island effect, urban heat-related disasters have become increasingly frequent<sup>74</sup>. Consistent with previous research, these regions have long been hotspots for frequent heatwaves, and the populations exposed to heatwaves are at very high and high risk of exposure. Therefore, when residents in these areas are frequently exposed to heatwaves, the negative impact of socio-economic factors deepens and the mental health of the population deteriorates.

Additionally, our results also revealed that as surface ozone concentrations increased, their correlation with mental health weakened, and when the number of heatwave days and events exceeded certain thresholds, residents' mental health improved. These phenomena may be attributed to China's unique governance model, which combines public "adaptive survival strategies" with governmental "systemic intervention measures"—a model developed over decades of practical experience in managing air pollution events. After prolonged exposure to air pollution and extreme events, residents undergo a psychological transition, moving from initial emotional resistance and avoidance to gradual acceptance and proactive coping. This process is accompanied by a reduction in psychological stress and relative emotional stabilization. Correspondingly, behavioral adaptation occurs, shifting from passive acceptance to active protective measures, including modifications in travel timing and modes, reduced outdoor activities, adoption of face masks, dietary adjustments, and optimization of indoor environments through air conditioning and air purification systems<sup>75,76</sup>. Concurrently, as the severity of air pollution and extreme events intensifies, governmental and public sectors have escalated policy interventions by implementing a suite of more targeted and efficacious countermeasures<sup>77</sup>. These interventions include issuing precise health warnings and protective guidance for vulnerable groups (such as children, the elderly, individuals with chronic diseases, and outdoor workers), upgrading urban infrastructure to improve the living environment, alleviating residents' economic burdens through financial subsidies and employment support<sup>78</sup>, establishing mental health shelters with professional psychological counseling services, enhancing the restoration of urban green spaces, supporting businesses in adopting telework policies to reduce outdoor exposure, and promoting community-based "cooling stations". In conclusion, understanding the mechanisms of ozone and heatwave impacts on residents' mental health is important for future policy formulation, implementation of interventions, and residents' coping preparedness and mindset.

### **Suggested measures for the impact of ozone and heatwaves on residents' mental health**

In response to the compounded impact of ozone and heatwave pollution on residents' mental health in China, and the regional differences discussed in the previous section, we propose a set of tiered and region-specific measures based on the mechanisms of pollution formation, geographical characteristics, and socio-economic conditions. These measures are outlined in the following three aspects.

**Strict Control of Pollution Emissions and Differentiated Regional Management.** For example, in South China, industrial emissions should be controlled, and key industries should be encouraged to use alternative

clean raw materials. A charge should be imposed on high-emission enterprises, and new high-rise buildings should be required to incorporate ventilation gaps, in alignment with prevailing wind directions, to reduce the urban heat island effect. North and East China focus on promoting regional energy structure transformation and controlling transport emissions. In western China, control measures for natural sources of volatile organic compounds (VOCs) should be implemented, such as planting low-volatility tree species and establishing wind and sand control forests along oasis edges to mitigate the enhancement of photochemical reactions by dust and sand.

**Strengthening Health Risk Prevention and Control with Multi-level Early Warning and Intervention.** A refined early warning system that integrates meteorological data, pollution monitoring, and hospital psychiatric outpatient data from different regions to achieve sub-regional early warning. Protection tips should be targeted to high-risk groups (such as outdoor workers, individuals with chronic diseases, etc.) through government apps, ensuring that preventive measures are appropriately disseminated.

**Enhancing the Role of Social Support Systems to Promote Environmental Equity and Resilience.** Improve the infrastructure of each region and carry out targeted renovation of old and small communities in densely populated areas. Upgrade social and public health services and provide timely psychological counseling to residents exposed to pollution. Strengthen climate mental health education in all regions, teaching psychological adjustment skills and emergency protection. Develop synergistic strategies for clean air and climate mitigation that provide significant environmental and climate co-benefits for sustainable development and protect the physical and mental health of the population.

In conclusion, we suggest that a comprehensive three-pronged approach—"pollution control, health protection, and social support"—can effectively mitigate the mental health risks posed by ozone and heatwave pollution.

### Research limitations and future directions

This study quantitatively analyzes the dual ozone-heatwave events and the mental health of the population in China, focusing on the spatiotemporal evolution characteristics of pollution and extreme events and their impacts. However, the mechanisms of the multiple impacts of surface ozone and heat waves on the mental health of the population need to be further investigated.

### Conclusion

This study investigated the spatiotemporal variations, population exposure risks, and impacts on residents' mental health due to summer surface ozone and heatwaves in China from 2013 to 2020. The findings indicate that ozone concentrations and heatwave occurrences initially increased and then decreased. Ozone levels rose from 85.98  $\mu\text{g}/\text{m}^3$  in 2013 to a peak of 105.33  $\mu\text{g}/\text{m}^3$  in 2019, before slightly dropping to 102.54  $\mu\text{g}/\text{m}^3$  in 2020. Similarly, heatwave days increased from 9.31 to 15.62 before decreasing to 11.76, and heatwave events followed a similar trend. Ozone concentrations increased in 96% of regions, notably in the Beijing-Tianjin-Hebei and Central Plains urban clusters, and were positively correlated with heatwaves across most areas. The proportion of the population exposed to high ozone levels surged from 0.19% in 2013 to 16.50% in 2020, while those experiencing more than 20 heatwave days annually increased from 13.71 to 24.17%. High-risk regions for ozone were concentrated in key urban clusters, while heatwaves were prominent in North, Central, and East China. Future risks of ozone and heatwave exposure are expected to persist in 57.95% and 20.91% of areas, respectively, with significant implications for mental health, particularly in high-risk urban areas.

### Data availability

The data that support the findings of this study are available on request from the corresponding author.

Received: 11 September 2024; Accepted: 29 May 2025

Published online: 01 July 2025

### References

1. Liu, C. et al. Interactive effects of ambient fine particulate matter and ozone on daily mortality in 372 cities: Two stage time series analysis. *BMJ* **383**, e075203 (2023).
2. Ma, Y. et al. Short-term effect of ambient ozone pollution on respiratory diseases in western China. *Environ. Geochem. Health* **44**, 4129–4140 (2022).
3. Wang, Y., Song, Q., Frei, M., Shao, Z. & Yang, L. Effects of elevated ozone, carbon dioxide, and the combination of both on the grain quality of Chinese hybrid rice. *Environ. Pollut.* **189**, 9–17 (2014).
4. Li, S., Wang, T., Zanis, P., Melas, D. & Zhuang, B. Impact of tropospheric ozone on summer climate in China. *J. Meteorol. Res.* **32**, 279–287 (2018).
5. Libonati, R. et al. Drought–heatwave nexus in Brazil and related impacts on health and fires: A comprehensive review. *Ann. N. Y. Acad. Sci.* **1517**(1), 44–62 (2022).
6. Symonds, M. Faculty opinions recommendation of IPCC, 2021: Summary for Policymakers. In: Climate Change 2021: The Physical Science Basis. Contribution of Working Group I to the Sixth Assessment Report of the Intergovernmental Panel on Climate Change. *Faculty Opinions – Post-Publication Peer Review of the Biomedical Literature* (2021).
7. Yuan, W. et al. Severe summer heatwave and drought strongly reduced carbon uptake in Southern China. *Sci. Rep.* **6**, 18813 (2016).
8. Chen, T., Wang, T., Xue, L. & Brasseur, G. Heatwave exacerbates air pollution in China through intertwined climate-energy-environment interactions. *Sci. Bull.* **69**, 2765–2775 (2024).
9. Xu, Z., Cheng, J., Hu, W. & Tong, S. Heatwave and health events: A systematic evaluation of different temperature indicators, heatwave intensities and durations. *Sci. Total Environ.* **630**, 679–689 (2018).
10. Zhou, W. et al. The effects of heatwave on cognitive impairment among older adults: Exploring the combined effects of air pollution and green space. *Sci. Total Environ.* **904**, 166534 (2023).
11. Zhou, W. et al. Heatwave exposure in relation to decreased sleep duration in older adults. *Environ. Int.* **183**, 108348 (2023).

12. Li, M. et al. Coping with the concurrent heatwaves and ozone extremes in China under a warming climate. *Sci. Bull.* **69**, 2938–2947 (2024).
13. Utembe, S. R. et al. Hot Summers: Effect of extreme temperatures on ozone in Sydney, Australia. *Atmosphere* **9**, 466 (2018).
14. Hertig, E., Russo, A. & Trigo, R. M. Heat and ozone pollution waves in Central and South Europe—Characteristics, weather types, and association with mortality. *Atmosphere* **11**, 1271 (2020).
15. Pyrgou, A., Hadjinicolaou, P. & Santamouris, M. Enhanced near-surface ozone under heatwave conditions in a Mediterranean island. *Sci. Rep.* **8**, 9191 (2018).
16. Wang, R. et al. The relationship between the intensified heat waves and deteriorated summertime ozone pollution in the Beijing–Tianjin–Hebei region, China, during 2013–2017. *Environ. Pollut.* **314**, 120256 (2022).
17. Cristofanelli, P. et al. Anomalous high ozone concentrations recorded at a high mountain station in Italy in summer 2003. *Atmos. Environ.* **41**, 1383–1394 (2006).
18. Gao, M. et al. Large-scale climate patterns offer preseasonal hints on the co-occurrence of heat wave and O<sub>3</sub> pollution in China. *Proc. Natl. Acad. Sci. U S A* **120**, 26 (2023).
19. Mohrén, V. A., Goldstein, W. & Wang, W.-C. Tropospheric ozone and climate change. *Air Waste* **43**, 1332–1334 (1993).
20. Lin, M. et al. Vegetation feedbacks during drought exacerbate ozone air pollution extremes in Europe. *Nat. Clim. Chang.* **10**, 444–451 (2020).
21. Zhang, J. et al. Impacts of compound extreme weather events on ozone in the present and future. *Atmos. Chem. Phys.* **18**, 9861–9877 (2018).
22. Yin, P. et al. Ambient ozone pollution and daily mortality: A nationwide study in 272 Chinese cities. *Environ. Health Perspect.* **125**, 117006 (2017).
23. Yang, Q., Peng, H. & Li, Q. Study on urban heatwave characteristics and thermal stress scenarios based on China's heatwave hazard zoning. *Urban Clim.* **55**, 101957 (2024).
24. Huang, Z. et al. Different characteristics of independent and compound extreme heat and ozone pollution events in the Greater Bay Area of China. *Int. J. Appl. Earth Obs. Geoinf.* **124**, 103508 (2023).
25. Lu, C. et al. An unusual high ozone event over the North and Northeast China during the record-breaking summer in 2018. *J. Environ. Sci.* **104**, 264–276 (2020).
26. Lu, X. et al. Rapid increases in Warm-Season surface ozone and resulting health impact in China since 2013. *Environ. Sci. Technol. Lett.* **7**, 240–247 (2020).
27. Schnell, J. L. & Prather, M. J. Co-occurrence of extremes in surface ozone, particulate matter, and temperature over eastern North America. *Proc. Natl. Acad. Sci.* **114**, 2854–2859 (2017).
28. Zhao, H., Zheng, Y., Li, T., Wei, L. & Guan, Q. Temporal and spatial variation in, and population exposure to, summertime Ground-Level ozone in Beijing. *Int. J. Environ. Res. Public Health* **15**, 628 (2018).
29. Wang, J. et al. Comparing relationships between urban heat exposure, ecological structure, and socio-economic patterns in Beijing and New York City. *Landsc. Urban Plan.* **235**, 104750 (2023).
30. Wang, Y. et al. Global future population exposure to heatwaves. *Environ. Int.* **178**, 108049 (2023).
31. Zhang, J. J., Wei, Y. & Fang, Z. Ozone pollution: A major health hazard worldwide. *Front. Immunol.* **10**, 2518 (2019).
32. Mitis, F., Iavarone, I. & Martuzzi, M. Health impact of ozone in 13 Italian cities. *PubMed* **31**, 323–332 (2008).
33. Campbell, S., Remenyi, T. A., White, C. J. & Johnston, F. H. Heatwave and health impact research: A global review. *Health Place* **53**, 210–218 (2018).
34. Arndal, M. F., Tolver, A., Larsen, K. S., Beier, C. & Schmidt, I. K. Fine root growth and vertical distribution in response to elevated CO<sub>2</sub>, warming and drought in a mixed Heathland-Grassland. *Ecosystems* **21**, 15–30 (2017).
35. Du, H. et al. Exposure to concurrent heatwaves and ozone pollution and associations with mortality risk: A nationwide study in China. *Environ. Health Perspect.* **132**, 047012 (2024).
36. Francis, X. V. et al. Mechanisms responsible for the build-up of ozone over South East England during the August 2003 heatwave. *Atmos. Environ.* **45**, 6880–6890 (2011).
37. Wang, Z., Zhu, L., Peng, M., Zheng, H. & Zhang, Y. Summer heatwave, ozone pollution and ischemic stroke mortality: An individual-level case-crossover study. *Environ. Res.* **268**, 120818 (2025).
38. Chen, H. et al. Projections of heatwave-attributable mortality under climate change and future population scenarios in China. *Lancet Reg. Health-West. Pac.* **28**, 100582 (2022).
39. King, J. D., Zhang, S. & Cohen, A. Air pollution and mental health: Associations, mechanisms and methods. *Curr. Opin. Psychiatry* **35**(3), 192–199 (2021).
40. Hautekiet, P. et al. Air pollution in association with mental and self-rated health and the mediating effect of physical activity. *Environ. Health* **21**, 29 (2022).
41. Zhang, G. et al. Heatwave-amplified atmospheric oxidation in a multi-province border area in Xuzhou, China. *Front. Environ. Sci.* **12**, 1496584 (2024).
42. Su, J., Jiao, L. & Xu, G. Intensified exposure to compound extreme heat and ozone pollution in summer across Chinese cities. *Npj Clim. Atmos. Sci.* **8**, 78 (2025).
43. Cao, Z., Zhou, J., Li, M., Huang, J. & Dou, D. Urbanites' mental health undermined by air pollution. *Nat. Sustain.* **6**, 470–478 (2023).
44. Xue, T. et al. Estimating spatiotemporal variation in ambient ozone exposure during 2013–2017 using a data-fusion model. *Environ. Sci. Technol.* **54**, 14877–14888 (2020).
45. Bai, K., Ma, M., Chang, N.-B. & Gao, W. Spatiotemporal trend analysis for fine particulate matter concentrations in China using high-resolution satellite-derived and ground-measured PM<sub>2.5</sub> data. *J. Environ. Manag.* **233**, 530–542 (2018).
46. Chen, Y. Reconstructing the mathematical process of spatial autocorrelation based on Moran's statistics. *Geogr. Res.* **28**(6), 1449–1463 (2009).
47. Yuanjian, Y. Effect of MAUP in spatial autocorrelation. *Acta Geogr. Sin.* **66**, 1597 (2011).
48. Wang, J. *Spatial Analysis* 76–84 (Science Press, 2006).
49. Li, F. & Hao, J. Study on the environmental risk assessment of the Yangtze River economic zone. *Resources and Environment in the Yangtze Basin*. (2018)
50. Aunan, K., Ma, Q., Lund, M. T. & Wang, S. Population-weighted exposure to PM<sub>2.5</sub> pollution in China: An integrated approach. *Environ. Int.* **120**, 111–120 (2018).
51. Wang, L., Rohli, R. V., Lin, Q., Jin, S. & Yan, X. Impact of extreme heatwaves on population exposure in China due to additional warming. *Sustainability* **14**, 11458 (2022).
52. Du, S. et al. Policy implications for synergistic management of PM<sub>2.5</sub> and O<sub>3</sub> pollution from a pattern-process-sustainability perspective in China. *Sci. Total. Environ.* **916**, 170210 (2024).
53. Wang, X., Li, T., Ikhumhen, H. O. & Sá, R. M. Spatio-temporal variability and persistence of PM<sub>2.5</sub> concentrations in China using trend analysis methods and Hurst exponent. *Atmos. Pollut. Res.* **13**, 101274 (2021).
54. Hou, X. et al. Character of vegetation cover change in China's Eastern Coastal Areas 1998–2008. *Sci. Geogr. Sin.* **30**(5), 735–741 (2010).
55. Wang, L. et al. Evolution of surface ozone pollution pattern in eastern China and its relationship with different intensity heatwaves. *Environ. Pollut.* **338**, 122725 (2023).

56. Liao, K.-J. et al. Current and future linked responses of ozone and PM<sub>2.5</sub> to emission controls. *Environ. Sci. Technol.* **42**, 4670–4675 (2008).
57. Wang, H. et al. Role of heat wave-induced biogenic VOC enhancements in persistent ozone episodes formation in Pearl River Delta. *J. Geophys. Res. Atmos.* **126**, e2020JD034317 (2021).
58. Kivimäki, M. et al. Association between socioeconomic status and the development of mental and physical health conditions in adulthood: A multi-cohort study. *Lancet Public Health* **5**, e140–e149 (2020).
59. Laaksonen, E. et al. Socioeconomic circumstances and common mental disorders among Finnish and British public sector employees: Evidence from the Helsinki Health Study and the Whitehall II Study. *Int. J. Epidemiol.* **36**, 776–786 (2007).
60. Najafi, F. et al. Decomposing socioeconomic inequality in poor mental health among Iranian adult population: Results from the PERSIAN cohort study. *BMC Psychiatry* **20**, 1 (2020).
61. Thomson, R. M. et al. How do income changes impact on mental health and wellbeing for working-age adults? A systematic review and meta-analysis. *Lancet Public Health* **7**(6), e515–e528 (2022).
62. Srivastava, K. Mental health and industry: Dynamics and perspectives. *Ind. Psychiatry J.* **18**, 1 (2009).
63. Gunn, L. D. Can a liveable city be a healthy city, now and into the future?. *Intern. Med. J.* **50**, 1405–1408 (2020).
64. Zumelzu, A. & Herrmann-Lunecke, M. G. Mental well-being and the influence of place: Conceptual approaches for the built environment for planning healthy and walkable Cities. *Sustainability* **13**, 6395 (2021).
65. Liu, H., Nong, H., Ren, H. & Liu, K. The effect of nature exposure, nature connectedness on mental well-being and ill-being in a general Chinese population. *Landsc. Urban Plan.* **222**, 104397 (2022).
66. Petersen, J. M. et al. Examining the promotion of mental health and wellbeing in Australian sports clubs. *Sport Educ. Soc.* 1–12 (2024).
67. Johnston, I. et al. Increasing access to psychological therapy on acute mental health wards: Staff and patient experiences of a stepped psychological intervention. *BMC Psychiatry* **25**, 300 (2025).
68. Chen, Q. et al. Digital empowerment in mental health: A meta-analysis of internet-based interventions for enhancing mental health literacy. *Int. J. Clin. Health Psychol.* **24**, 100489 (2024).
69. Thompson, R. et al. Air pollution, traffic noise, mental health, and cognitive development: A multi-exposure longitudinal study of London adolescents in the SCAMP cohort. *Environ. Int.* **191**, 108963 (2024).
70. Wang, J.-Y. Mental health policy reform and service delivery in England. *BMJ Open* **18**, 143–180 (2014).
71. Liu, D. et al. Spatio-temporal patterns and population exposure risks of urban heat island in megacity Shanghai, China. *Sustain. Cities Soc.* **108**, 105500 (2024).
72. Vujovic, S., Haddad, B., Karaky, H., Sebaibi, N. & Boutouil, M. Urban heat island: Causes, consequences, and mitigation measures with emphasis on reflective and permeable pavements. *CivilEng* **2**(2), 459–484 (2021).
73. Youfei, Z., Xuesong, D., Rongjun, W. & Jifu, Y. Temporal and spatial feature analyses of summer high temperature and heat wave in Jiangsu Province in past 50 years. *Ziran Zaihai Xuebao* **21**, 43–50 (2012).
74. Chew, L. W., Liu, X., Li, X.-X. & Norford, L. K. Interaction between heat wave and urban heat island: A case study in a tropical coastal city, Singapore. *Atmos. Res.* **247**, 105134 (2020).
75. Zhang, X., Chen, F. & Chen, Z. Heatwave and mental health. *J. Environ. Manag.* **332**, 117385 (2023).
76. Yang, Z. et al. Air pollution and mental health: The moderator effect of health behaviors. *Environ. Res. Lett.* **16**, 044005 (2021).
77. Buscail, C., Upegui, E. & Viel, J.-F. Mapping heatwave health risk at the community level for public health action. *Int. J. Health Geogr.* **11**, 1 (2012).
78. Song, Y., Li, M., Zhang, M. & Sun, X. Study on the impact of air pollution control on urban residents' happiness from microscopic perspective. *J. Clean. Prod.* **229**, 1307–1318 (2019).

## Author contributions

Z.R.: Investigation, Software, Visualization and Writing-original draft. Z.J. and H.Y.: Supervision. C.L. and D.S.: Software. H.C.: Conceptualization, Supervision and Writing-review & editing. All authors reviewed the manuscript.

## Declarations

## Competing interests

The authors declare no competing interests.

## Additional information

**Supplementary Information** The online version contains supplementary material available at <https://doi.org/10.1038/s41598-025-04930-4>.

**Correspondence** and requests for materials should be addressed to J.Z. or C.H.

**Reprints and permissions information** is available at [www.nature.com/reprints](http://www.nature.com/reprints).

**Publisher's note** Springer Nature remains neutral with regard to jurisdictional claims in published maps and institutional affiliations.

**Open Access** This article is licensed under a Creative Commons Attribution-NonCommercial-NoDerivatives 4.0 International License, which permits any non-commercial use, sharing, distribution and reproduction in any medium or format, as long as you give appropriate credit to the original author(s) and the source, provide a link to the Creative Commons licence, and indicate if you modified the licensed material. You do not have permission under this licence to share adapted material derived from this article or parts of it. The images or other third party material in this article are included in the article's Creative Commons licence, unless indicated otherwise in a credit line to the material. If material is not included in the article's Creative Commons licence and your intended use is not permitted by statutory regulation or exceeds the permitted use, you will need to obtain permission directly from the copyright holder. To view a copy of this licence, visit <http://creativecommons.org/licenses/by-nc-nd/4.0/>.

© The Author(s) 2025